*Pure Appl. Chem.*, Vol. 78, No. 8, pp. 1505–1518, 2006.
doi:10.1351/pac200678081505


# Structures and functions of carotenoids bound to reaction centers from purple photosynthetic bacteria*

Hideki Hashimoto[1,2,‡], Ritsuko Fujii[1], Kazuhiro Yanagi[1], Toshiyuki Kusumoto[1], Alastair T. Gardiner[3], Richard J. Cogdell[3], Aleksander W. Roszak[4], Neil W. Issacs[4], Zeus Pendon[5], Dariusz Niedzwiedski[5], and Harry A. Frank[5]

*[1]Department of Physics, Graduate School of Science, Osaka City University, 3-3-138 Sugimoto, Sumiyoshi-ku, Osaka 558-8585, Japan; [2]"Light and Control", PRESTO, Japan Science and Technology Agency, 4-1-8 Honcho Kawaguchi, Saitama 332-0012, Japan; [3]Division of Biochemistry and Molecular Biology, IBLS, University of Glasgow, Glasgow G12 8QQ, Scotland, UK; [4]Department of Chemistry, Joseph Black Building, University of Glasgow, Glasgow G12 8QQ, Scotland, UK; [5]Department of Chemistry, U-3060, University of Connecticut, Storrs, CT 06269-3060, USA*

*Abstract*: The photoprotective function of 15,15'-*cis*-carotenoids bound to the photosynthetic reaction centers (RCs) of purple bacteria has been studied using carotenoids reconstituted into carotenoidless RCs from *Rhodobacter sphaeroides* strain R26.1. The triplet-energy level of the carotenoid has been proposed to affect the quenching of the triplet state of special-pair bacteriochlorophyll (P). This was investigated using microsecond flash photolysis to detect the carotenoid triplets as a function of the number of conjugated double bonds, $n$. The carotenoid triplet signals were extracted by using singular-value decomposition (SVD) of the huge matrices data, and were confirmed for those having $n$ = 8 to 11. This interpretation assumes that the reconstituted carotenoids occupy the same binding site in the RC. We have been able to confirm this assumption using X-ray crystallography to determine the structures of carotenoidless, wild-type carotenoid-containing, and 3,4-dihydro-spheroidene-reconstituted RCs. The X-ray study also emphasized the importance of the methoxy group of the carotenoids for binding to the RCs. Electroabsorption (Stark) spectroscopy was used to investigate the effect of the carotenoid on the electrostatic field around P. This electrostatic field changed by 10 % in the presence of the carotenoid.

*Keywords*: carotenoids; reaction centers; X-ray crystallography; Stark spectroscopy; transient absorption; triplet state; photoprotection; spheroidene analogs.

## INTRODUCTION

The 3D structure of the purple bacterial reaction center (RC) from *Blastochloris (Blc.) viridis*, formerly *Rhodopseudomonas (Rps.) viridis*, was first determined by Deisenhofer et al. [1]. This was followed by

*Paper based on a presentation at the 14th International Symposium on Carotenoids, Edinburgh, Scotland, 17–22 July 2005. Other presentations are published in this issue, pp. 1477–1557.

‡Corresponding author: E-mail: hassy@sci.osaka-cu.ac.jp

the determination of the structure of the RC from *Rhodobacter* (*Rba.*) *sphaeroides* [2–11]. Figure 1 shows the arrangement of the pigments in the RC of *Rba. sphaeroides* [12]. The RC is composed of H, L, and M subunits, a special pair of bacteriochlorophylls (BChl) (P), two accessory monomeric BChls ($B_A$ and $B_B$), two monomeric bacteriopheophytins ($H_A$ and $H_B$), and two quinones ($Q_A$ and $Q_B$) are bound to the L and M subunits with pseudo two-hold symmetry. After excitation energy is transferred from the antenna system to the RC, an electron is transferred from P to $H_A$ and then onto $Q_A$. If excess light energy is supplied to the RC, a triplet excited-state of P ($^3$P) is generated. The presence of $^3$P can result in the production of harmful singlet oxygen [13].

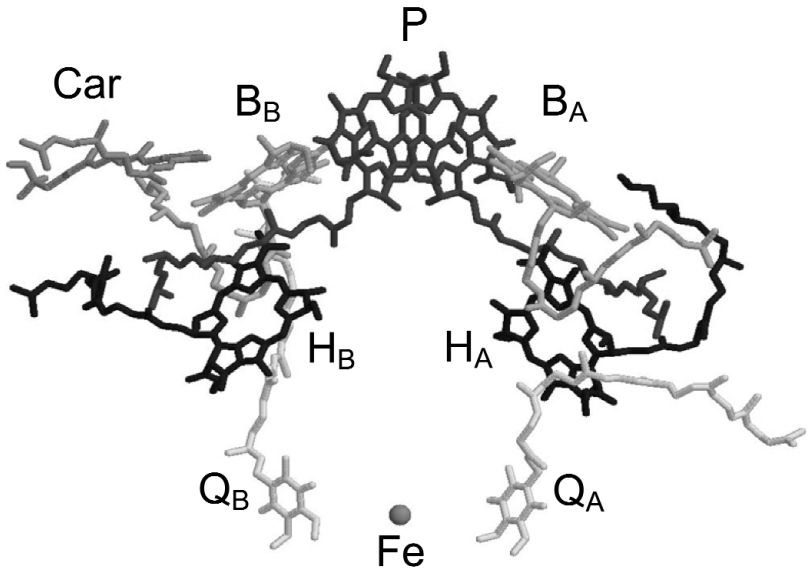


**Fig. 1** Pigment arrangement in the RC from *Rba. sphaeroides* 2.4.1 (PDB ID:1PCR).

A 15,15'-*cis*-carotenoid bound to the B-branch serves a photoprotective function by quenching $^3$P through a triplet-triplet energy transfer reaction that produces triplet excited carotenoid [13]. A monomeric BChl in B-side ($B_B$) has been reported to mediate the triplet-energy transfer from P to carotenoid [14], although the triplet-energy of $B_B$ is ~140 cm$^{-1}$ higher than that of P [15]. The detailed mechanism of the photoprotective function of the RC-bound carotenoid has been further studied using carotenoids reconstituted into carotenoidless RCs from *Rba. sphaeroides* R26.1 [16]. It was concluded that the triplet-energy levels of carotenoids having a number of conjugated double bonds ($n$) less than 10 are higher than that of $B_B$, since neither transient absorption nor electron paramagnetic resonance (EPR) signals from the triplet carotenoids could be detected in carotenoidless RC into which carotenoids with $n$ = 8 or 9 conjugated double bonds had been incorporated [16]. However, this assumes that all of these reconstituted carotenoids occupy the same binding site as in the wild-type RCs.

In this paper, we first describe our recent work on the structures of carotenoids incorporated into the carotenoidless RC from *Rba. sphaeroides* R26.1 determined by X-ray crystallography [12]. In addition, the effect of the reconstituted carotenoid on the electrostatic environment of P has been investigated using electroabsorption (Stark) spectroscopy [17]. Finally, some new data is presented that demonstrates that carotenoids with 8 or 9 conjugated double bonds also quench $^3$P.

## STRUCTURES OF CAROTENOIDS INCORPORATED INTO CAROTENOIDLESS REACTION CENTERS AS DETERMINED BY X-RAY CRYSTALLOGARPHY

X-ray diffraction was used to determine high-resolution structures of the carotenoidless RCs from *Rba. sphaeroides* R26.1, without or reconstituted with carotenoids [12]. The results are compared with the structure of the RC from a semiaerobically grown *Rba. sphaeroides* mutant strain AM260W of strain 2.4.1-containing spheroidenone (PDB ID code 1QOV) [10], which shows the useful enough resolution (2.1 Å resolution) of an RC which naturally contains a carotenoid. The present study (see below) shows that, within the limits of the resolutions of these structures, the reconstituted carotenoid occupies the same binding site as in the wild-type RC, adopts the same 15,15'-*cis*-configuration as in the wild-type RC, and has the same major interactions with the protein in the binding site as in the wild-type RC. Interestingly comparison of the "reconstituted" RC structure with the carotenoidless RC revealed a novel mechanism by which the carotenoid binds to the protein unidirectionally in its characteristic 15,15'-*cis*-configuration. This information is important for understanding how the protein controls the efficiency of triplet-energy transfer from P to the carotenoid.

Figure 2 shows four spheroidene analogs, all having a methoxy group, that were reconstituted into the RC. The spheroidene analogs with longer ($n$ = 11) and shorter ($n$ = 9 and 8) conjugated chains than spheroidene ($n$ = 10) were synthesized systematically as reported previously [18]. High-resolution structures were obtained for the RC from the R26.1 RC and those reconstituted with spheroidene and 3,4-dihydrospherodene (PDB codes are 1RG5, 1RGN, and 1RQK, respectively).

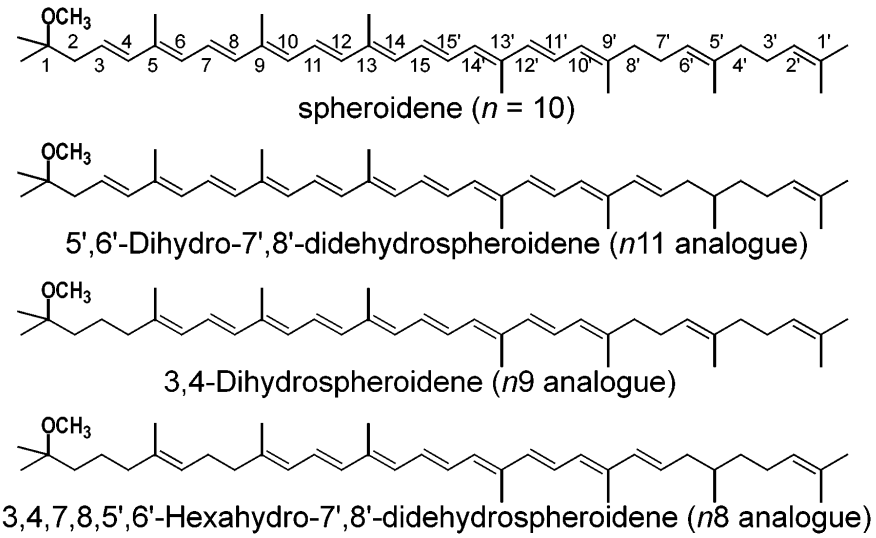


**Fig. 2** Chemical structures of three spheroidene analogs with spheroidene for comparison.

Figure 3A shows the entire carotenoid binding site and the relevant electron density for the AM260W mutant [12]. Both ends of carotenoid molecule in the RCs are solvent accessible in the crystal structure, but these areas constitute only about 15 % of the carotenoid's surface. The hydrophilic methoxy head of spheroidenone is involved in a single carotenoid-protein hydrogen-bonding interaction formed between the methoxy oxygen of carotenoid and the hydrogen on the indole group N atom of Trp M75 (not shown in Fig. 3). The $O_{Car}$–$N_{M75}$ distance was found to be 3.3 Å for spheroidenone, 2.9 Å for spheroidene, and 3.4 Å for 3,4-dihydrospheroidene. The hydrogen bond involving Trp M75 is probably the most energetically stable single protein contact for carotenoid binding, and as suggested by previous structures [4,10,19], it is very important for "locking" the carotenoid in its site and ensur-

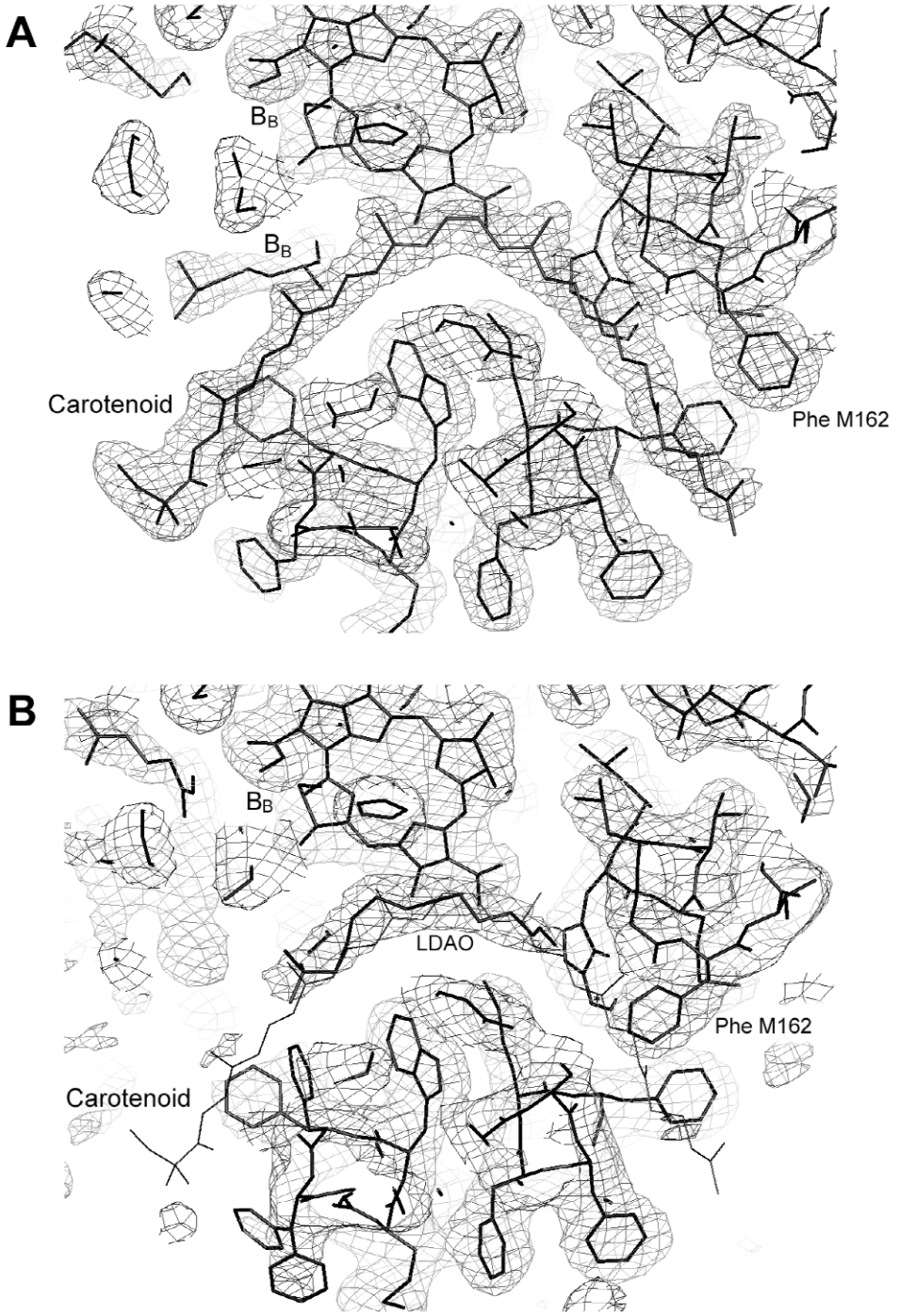


**Fig. 3** The carotenoid-binding site showing (A) the electron density for the AM260W mutant of *Rba. sphaeroides* containing spheroidenone [10] and (B) the electron density and structure of the RC from the carotenoidless mutant *Rba. sphaeroides* R-26.1 in the absence of a bound carotenoid overlaid with the structure of spheroidenone. Note that when the carotenoid is absent (in [B]), the binding site contains a single LDAO detergent molecule and the "gatekeeper" Phe M162 side chain. This conformation of Phe M162 contrasts with that shown in (A), where, in the presence of the carotenoid, it is found in an alternate position outside the binding site (PDB ID: 1QOV).

ing secure, unidirectional binding. This idea is supported by the technical observation that carotenoids lacking the methoxy group are often easily removed during purification of the RCs.

Figure 3B shows the carotenoid-binding site with the electron density for the carotenoidless RC of R26.1 overlaid with spheroidenone from AM260W RC [12]. When the carotenoid is absent, its binding pocket is found to be smaller because the $B_B$ phytol tail adopts a different conformation directed away from the carotenoid site. This changes the shape of approximately one-third of the binding pocket from a tunnel to a solvent-accessible channel. The central portion of the pocket contains a stretch of electron density, which can be fitted with a single LDAO detergent molecule. The carotenoid tail region of the pocket space has new electron density, which clearly indicates an alternative conformation of the Phe M162 to that found in carotenoid-containing RCs. This is the most expected conformation for phenylalanine side chains, being found in ~46 % of phenylalanine residues in high-resolution protein structures [20]. However, as clearly shown in Fig. 3B, this conformation would clash sterically with the carotenoid when it is also present in the binding site. In the presence of the carotenoid, the phenylalanine side chain is rotated out of the binding site (Fig. 3A). Thus, Phe M162 acts as a "gatekeeper" residue, preserving the integrity and structure of the binding site in the absence of the carotenoid, yet having the ability to change its conformation and move away from the site when the carotenoid is presented for binding.

In the vicinity of the carotenoid-binding site, the structures of main-chain atoms of the protein are, within the limits of the crystallographic resolution, identical in structures of the three carotenoid-containing RCs. As shown in Fig. 4, the conformations of the three carotenoids only differ slightly at the nonconjugated tail region and in the methoxy head area. It is important to note that the close agreement in the structures shown in Fig. 4 derives from overlaying the surrounding M chain protein and not from superimposing the carotenoid molecules themselves. Thus, it is clear that the 15,15'-*cis*-bond is in an identical position relative to the $B_B$ macrocycle in both natural and carotenoid-reconstituted structures. The methoxy group of the spheroidene molecule was found to be rotated by 180° relative to its orientation in the other two structures but still forming a hydrogen bond to the hydrogen on the indole N of the Trp M75. The crystal structures presented here show that reconstitution of spheroidene and 3,4-dihydrospheroidene into the RCs from *Rba. sphaeroides* R26.1 lead to carotenoid binding that is very similar to that found for natural spheroidenone in the RC. Most importantly, the position of the characteristic 15,15'-*cis*-bond of the carotenoid relative to the $B_B$ macrocycle is virtually identical in all cases and is in close proximity to it, as is required for triplet–triplet energy transfer from P to the carotenoid via $B_B$ [21].

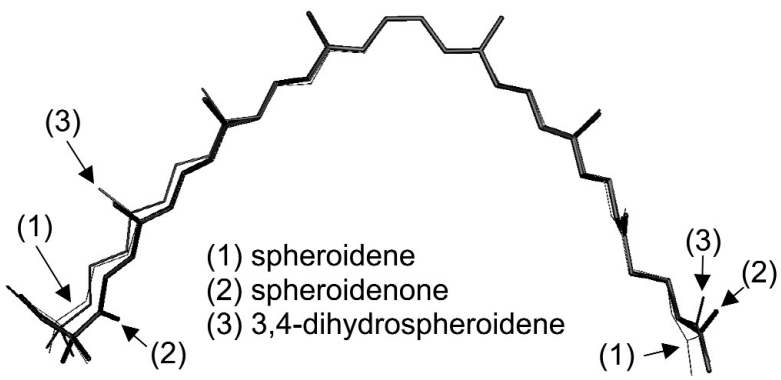


**Fig. 4** The three carotenoid structures overlaid by matching the surrounding M chain protein of the RC proteins: The circles near the ends of the carotenoids correspond to oxygen atoms. Spheroidenone was present in RCs from the semiaerobically grown cells, whereas spheroidenone and 3,4-dihydrosperoidene were reconstituted into RCs isolated from R26.1.

The structure of the carotenoid-binding site elucidated from the present studies provides a likely scenario for the path the carotenoid must take upon incorporation into protein. The carotenoid must enter the protein from the Trp M75 side; otherwise, Phe M162, in its preferred conformation in the empty carotenoid-binding site (Fig. 3B), would not be able to move out the way. Moreover, the bulkiness of the methoxy head group suggests that the floppy tail of the carotenoid must be inserted first upon reconstitution. The carotenoid pushes past the gatekeeper residue, Phe M162, and is then fixed in place by hydrogen-bonding interaction between the methoxy group of the carotenoid and the hydrogen on the indole N on the locking residue, Trp M75.

## LOCAL ELECTROSTATIC FIELD INDUCED BY THE CAROTENOID BOUND TO THE REACTION CENTER OF *Rba. sphaeroides*

A 15,15'-*cis*-carotenoid is located ~11 Å from P on the non-electron-transferring B-branch [11,12,22]. As shown above, since the distance between the 15,15'-*cis*-double bond of carotenoid and $B_B$ is 3.2~3.4 Å, carotenoid is in van der Waals contact with $B_B$ [12]. Singlet excitation energy is transfered from carotenoid to P through $B_B$ [23], whereas triplet excitation energy is transfered from P to carotenoid through $B_B$ [14]. The former process is thought to correspond to the light-harvesting function of carotenoid (observed also in LH complexes) since carotenoid absorbs light in the spectral region, 400–600 nm, where BChls have weak absorption. The latter process reflects the photoprotective function of carotenoid, as this transfer process prevents the generation of harmful singlet oxygen [24]. Although the mechanisms of these two functions of the carotenoid have been well investigated [13,25], a possible role of the carotenoid in promoting unidirectional electron transfer along A-branch has received scant attention. It appears that carotenoid does not directly impinge on electron transfer, rather unidirectional electron transfer occurs regardless of the presence of carotenoid [26]. However, it should be noted that carotenoid is the only one pigment that apparently breaks the pseudo two-fold symmetry of the RC and that unidirectional electron transfer basically results from asymmetry in the pigment-protein interactions. Therefore, it is interesting to ask whether the asymmetry induced by the presence of the carotenoid could also contribute to the asymmetry in the electrostatic environment around the pigments between the A and B branches and as a consequence "indirectly" affects the electron-transfer process?

Nonlinear optical responses of materials are sensitive to the change of the local electrostatic environment [27]. Stark spectroscopy is one of the most promising methods to determine nonlinear optical parameters. Three nonlinear optical parameters can be determined from Stark spectroscopy [28,29]; (1) the transition dipole-moment polarizability and its hyperpolarizability (*D* factor), (2) the change of polarizability upon photoexcitation ($\Delta\alpha$), and (3) the change of dipole-moment upon photoexcitation ($\Delta\mu$). Stark spectroscopy has been extensively applied to the studies of RCs since the early 1980s [27,30–45] (for excellent reviews by Boxer et al., see [46,47]). The most remarkable characteristic of the nonlinear optical properties of the RC can be found in its large $\Delta\mu$ value of P. This is initially assumed to be caused by mixing with a charge-transfer (CT) state [37–39]. However, Middendorf et al. [27] pointed out that a strong local electric field can also induce such an enhancement of $\Delta\mu$. They estimated that the local electric field around P to be more than $1.2 \times 10^6$ [V/cm] [27] and proposed that the amplitude of the local electric field could be evaluated from the nonlinear optical parameters determined by Stark spectroscopy. Therefore, any change of the electric field due to the presence of carotenoid around P could in principle also be detected by comparing the nonlinear optical parameters of the RC-containing (R26.1 RC + Car) and -lacking carotenoid (R26.1 RC). In order to test this hypothesis, the Stark spectra of these two RC samples were determined.

### Theoretical model to analyze the Stark spectra

Although the general theory of Stark spectroscopy is relatively well developed [28,29], a fuller theoretical understanding of it within the biological context is required. This is needed in order to facilitate correlation of the measured spectra with the structure of the pigment-protein interactions and how these affect the magnitude of the experimentally determined nonlinear optical parameters (*D* factor, $\Delta\alpha$ and $\Delta\mu$). The present study has investigated the change in the electrostatic field around the RC pigments induced by the presence of carotenoid and its affect on the optical nonlinearity of these pigments. In order to study these effects, a theoretical model has been developed based on the background theory originally described by Liptay [28,29].

The ground and excited states of a pigment are denoted as $|0\rangle$ and $|1\rangle$, respectively. The electric field, **F**, affecting the electronic state of P is considered as a linear combination of the three vector components of the applied electric field ($\mathbf{F}_a$), the pocket field due to the presence of apoproteins ($\mathbf{F}_p$), and the electrostatic field induced by the presence of carotenoid ($\mathbf{F}_c$) [48]

$$\mathbf{F} = \mathbf{F}_a + \mathbf{F}_p + \mathbf{F}_c \tag{1}$$

Although the idea to describe the electrostatic field as a summation of the applied and pocket fields has already been suggested [48], the $\mathbf{F}_c$ term has been introduced additionally in order to clarify the effect of the presence of carotenoid.

According to eq. 1, the shift of the $|0\rangle \rightarrow |1\rangle$ transition energy induced by the electrostatic field (Stark shift), $\Delta\nu_{01}$, is written as [48]

$$\begin{aligned} h\Delta\nu_{01} &= -\Delta\boldsymbol{\mu}\mathbf{F} - \frac{1}{2}\Delta\boldsymbol{\alpha}\mathbf{F}^2 \\ &= -\Delta\boldsymbol{\mu}^*\mathbf{F}_a - \frac{1}{2}\Delta\boldsymbol{\alpha}\mathbf{F}_a^2 - \left(\Delta\boldsymbol{\mu} + \Delta\boldsymbol{\alpha}\mathbf{F}_p\right)\mathbf{F}_c - \frac{1}{2}\Delta\boldsymbol{\alpha}\mathbf{F}_c^2 - \Delta\boldsymbol{\mu}\mathbf{F}_p - \frac{1}{2}\Delta\boldsymbol{\alpha}\mathbf{F}_p^2 \end{aligned} \tag{2}$$

$$\Delta\boldsymbol{\mu}^* = \Delta\boldsymbol{\mu} + \Delta\boldsymbol{\alpha}\left(\mathbf{F}_p + \mathbf{F}_c\right) \tag{3}$$

It should be noted that the $\mathbf{F}_c$ term affects the transition frequency directly. According to eq. 2, the shift of the transition energy due to $\mathbf{F}_c$, $h\Delta_c\nu_{01}$, can be written as

$$h\Delta_c\nu_{01} = -\left(\Delta\boldsymbol{\mu} + \mathbf{F}_p\Delta\boldsymbol{\alpha}\right)\mathbf{F}_c \tag{4}$$

The transition dipole-moment between the ground and excited states in the presence of the electrostatic field, $\tilde{\boldsymbol{\mu}}_{01}$, can be written as

$$\tilde{\boldsymbol{\mu}}_{01} = \boldsymbol{\mu}_{01} + \mathbf{XF} + \frac{1}{2}\mathbf{YF}^2 \approx \boldsymbol{\mu}_{01} + \mathbf{XF}_a + \frac{1}{2}\mathbf{YF}_a^2 \tag{5}$$

Here, $\boldsymbol{\mu}_{01}$ is the transition dipole-moment in the absence of electrostatic field. **X** and **Y** are transition dipole-moment polarizability and hyper-polarizability (*D* factor) in the absence of the electrostatic field.

In this study, the RC was isotropically dispersed and fixed in a poly(vinyl alcohol) (PVA) polymer matrix and then the magic-angle technique was applied. After averaging over the whole ensemble of sample orientations, the absorption change due to the applied electric field $\mathbf{F}_a$, $\Delta A$, can be written as [49]

$$\Delta A = \left(\frac{1}{3}DA + \frac{1}{6}F\frac{dA/\nu}{d\nu} + \frac{1}{6}\left|\Delta\boldsymbol{\mu}^*\right|^2\frac{d^2A/\nu}{d\nu^2}\right)\left|\mathbf{F}_a\right|^2 \tag{6}$$

$$D = \frac{1}{\left|\boldsymbol{\mu}_{01}\right|^2}\left(\mathbf{X}^2 + \boldsymbol{\mu}_{01}\mathbf{Y}\right) \tag{7}$$

$$F = Tr\left[\boldsymbol{\Delta\alpha}\right] + 2\frac{\boldsymbol{\mu}_{01}\mathbf{X}}{\left|\boldsymbol{\mu}_{01}\right|^2}\boldsymbol{\Delta\mu}^* \approx Tr\left[\boldsymbol{\Delta\alpha}\right] \tag{8}$$

Equation 6 indicates that $\Delta A$ can be written as a linear combination of the zero, first-, and second-order derivatives of $A$. This equation corresponds to the theoretical formulation of $\Delta A$ developed by Liptay [29], except that $\boldsymbol{\Delta\mu}$ is replaced with $\boldsymbol{\Delta\mu}^*$. In eq. 8, it is assumed that $\boldsymbol{\Delta\alpha}$ will be the dominant contribution to the $F$ value since the contribution of the $D$ factor to the optical nonlinearity is expected to be small ($\mathbf{X} \sim 0$) [27].

There are two important implications from eq. 6: the coefficients of the zero- and first-order derivative components (the $D$ and $Tr[\boldsymbol{\Delta\alpha}]$ values) are not affected by $\mathbf{F}_c$ and the coefficient of the second-order derivative ($\boldsymbol{\Delta\mu}^*$) depends on the $\mathbf{F}_c$ value.

According to eq. 3, the change of the $\boldsymbol{\Delta\mu}^*$ value due to the presence of $\mathbf{F}_c$ ($\boldsymbol{\Delta}_c\boldsymbol{\mu}^*$) can be written as

$$\boldsymbol{\Delta}_c\boldsymbol{\mu}^* = \boldsymbol{\Delta\alpha}\mathbf{F}_c \tag{9}$$

Therefore, the $\boldsymbol{\Delta}_c\boldsymbol{\mu}^*$ value can be determined from the difference of $\boldsymbol{\Delta\mu}^*$ values between the carotenoidless and the carotenoid-containing RCs. Since the $\boldsymbol{\Delta\alpha}$ value can be also estimated from the Stark spectra, the magnitude of $\mathbf{F}_c$ can be quantitatively evaluated by using eq. 9.

To determine the values of $D$, $Tr[\boldsymbol{\Delta\alpha}]$, and $\boldsymbol{\Delta\mu}^*$, a multiregression analysis was used to simulate the waveforms of the Stark spectra using a linear combination of the zero-, first-, and second-order derivatives of the absorption spectra (hereafter called waveform analysis).

### Nonlinear optical parameters of P, B, and H bands determined by Stark spectroscopy

Figure 5 shows the observed absorption spectrum of R26.1 RC (solid line) at 293 K. The P, B, and H bands (dotted lines) were deconvoluted from the full spectrum using Gaussian functions. Figures 5b and 5c show the in-phase Stark spectra of R26.1 RC and R26.1 RC + Car at 293 K. Since the P, B, and H bands are expected to have different optical nonlinearity [39], the Stark spectra were reproduced by using linear combinations of the zero-, first-, and second-order derivatives of each separate absorption band. The difference spectrum between Figs. 5b and 5c is shown in Fig. 5d. A significant difference between the Stark spectra of the two RCs could be observed. This difference spectrum, in the region of the P band, resembles the second-order derivative form and indicates that the $\boldsymbol{\Delta\mu}^*$ values are different between the two RCs.

Figures 5e and 5f show the quadrature-phase Stark spectra of R26.1 RC and R26.1 RC + Car at 293 K. In contrast to the case at 79 K, quadrature-phase signals were observed at 293 K. At this temperature the presence of the phase-retarded signal indicates the presence of an electrostatic interaction between pigments and their surrounding protein environment [41]. Figure 5g shows the difference Stark spectrum between Figs. 5e and 5f. A small difference between the two RCs was observed and reflects the fact that the carotenoid induced a change in the electrostatic environment of P.

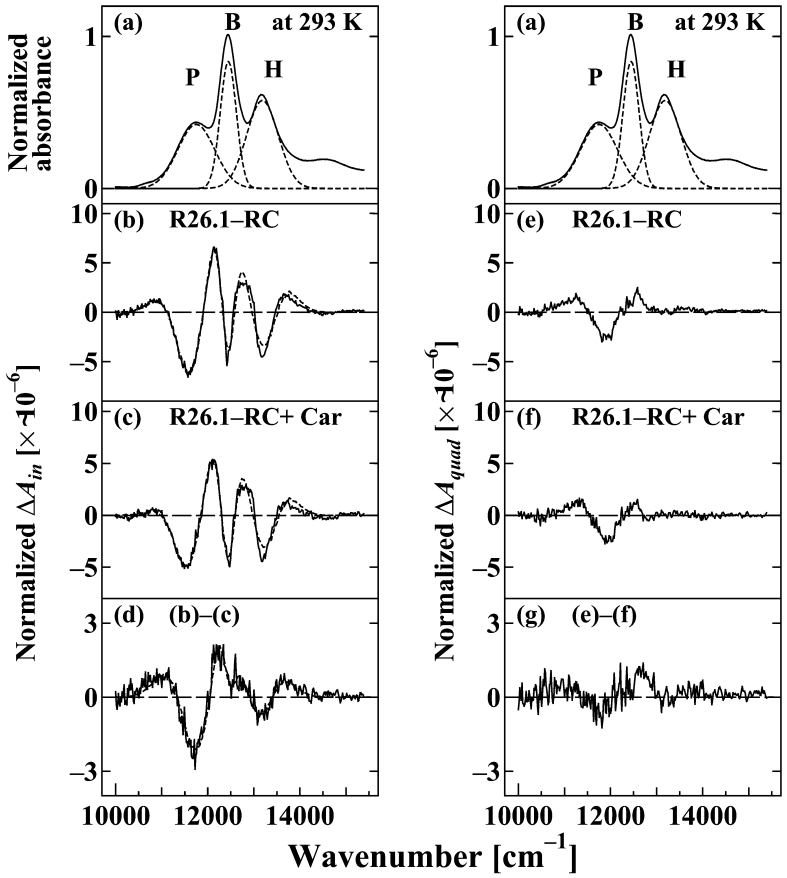


**Fig. 5** In- and quadrature-phase Stark spectra of R26.1 RC and R26.1 RC + Carat 293 K [17]. Panel a shows absorption spectrum (solid lines) of R26.1 RC and the P, B, and H bands determined from the deconvolution by using Gaussian functions (dotted lines). Panels b and c show the in-phase Stark spectra (solid lines) of R26.1 RC and R26.1 RC + Car and the results of waveform analyses (dotted lines). After the normalization procedure, the differential Stark spectra (d), between panels b and c were derived. Panels e and f show the quadrature-phase Stark spectra (solid lines) of R26.1 RC and R26.1 RC + Car. After the normalization procedure, the differential Stark spectrum (g), between panels e and f was derived.

The nonlinear optical parameters of the P, B, and H bands determined from the Stark spectra are summarized in Table 1. The most remarkable features present in Table 1 are the values of $\mathbf{\Delta\mu}^*$ of the P and B bands at 293 K. Even allowing for experimental error, there are significant differences in these values between the two RCs. According to eq. 9, this result clearly indicates the effect of $\mathbf{F}_c$ on the $\mathbf{\Delta\mu}^*$ values of the P and B bands. Only the nonlinear optical properties of the P band are discussed in detail here. There is about 1.0 [D/$f_L$] difference between the two RCs in the $\mathbf{\Delta\mu}^*$ values at 293 K and, according to eq. 9, this difference corresponds to $\mathbf{\Delta}_c\mathbf{\mu}$. Based on eq. 9, using the $Tr[\mathbf{\Delta\alpha}]$ value of $-2.1 \times 10^3$ [Å$^3$/$f_L{}^2$] at 293 K the $\mathbf{F}_c$ value was estimated to be $1.7 \times 10^5$ [V/cm]. In this calculation, the experimental error is taken into account for the minimum order estimation of $\mathbf{F}_c$ and the reported $f_L$ value of 1.2 was used [37,38]. The magnitude of the local field around P has been reported to be more than $1.2 \times 10^6$ [V/cm] [27]. Thus, the present result indicates that the presence of carotenoid induces up to a 10 % change of the electrostatic environment around P.

**Table 1** Nonlinear optical parameters determined from the waveform analyses of Stark spectra.

| | P band | $D$ [$10^{-18}$ [(m/$f_L$V)$^2$]] | Tr[Δα][Å$^3$/$f_L{}^2$] | Δμ* [D/$f_L$] |
|---|---|---|---|---|
| 79 K | R26.1-RC | –1.5 ± 0.4 | (2.2 ± 0.3) × 102 | 6.5 ± 0.3 |
| | R26.1-RC + Car | –1.8 ± 0.4 | (2.4 ± 0.8) × 102 | 6.5 ± 0.5 |
| 293 K | R26.1-RC | 3.9 ± 0.4 | –(1.7 ± 0.1) × 103 | 10.8 ± 0.4 |
| | R26.1-RC + Car | 3.6 ± 0.5 | –(1.7 ± 0.4) × 103 | 9.0 ± 0.4 |
| B band | $D$ [$10^{-18}$ [(m/$f_L$V)$^2$]] | Tr[Δα][Å$^3$/$f_L{}^2$] | Δμ* [D/$f_L$] | |
| 79 K | R26.1-RC | 0.9 ± 0.2 | –(1.2 ± 0.4) × 102 | 2.8 ± 0.3 |
| | R26.1-RC + Car | 1.4 ± 0.5 | –(1.1 ± 0.2) × 102 | 2.9 ± 0.2 |
| 293 K | R26.1-RC | –7.1 ± 0.5 | –(5.3 ± 3.6) × 10 | 2.1 ± 0.1 |
| | R26.1-RC + Car | –7.0 ± 1.7 | –(5.8 ± 2.4) × 10 | 1.5 ± 0.2 |
| H band | $D$ [$10^{-18}$ [(m/$f_L$V)$^2$]] | Tr[Δα][Å$^3$/$f_L{}^2$] | Δμ* [D/$f_L$] | |
| 79 K | R26.1-RC | 0.4 ± 0.2 | –(8.4 ± 7.2) × 10 | 4.4 ± 0.3 |
| | R26.1-RC + Car | 0.4 ± 0.1 | –(0.9 ± 2.0) × 10 | 4.3 ± 0.3 |
| 293 K | R26.1-RC | 0.8 ± 0.2 | (9.5 ± 2.3) × 10 | 6.2 ± 0.4 |
| | R26.1-RC + Car | 0.8 ± 0.3 | (10.0 ± 4.0) × 10 | 5.7 ± 0.5 |

X-ray crystallography of R26.1 RC and R26.1 RC + Car has shown that the difference between these RCs structurally is not simply the presence or absence of carotenoid: as shown in the previous section conformational changes of the phytol tail and/or individual amino acid residues also occur. The difference in the strength of the electrostatic field experienced by P and $B_B$ in R26.1 RC and R26.1 RC + Car is due to the presence or absence of carotenoid. However, it is not yet possible to distinguish between a direct interaction between carotenoid and P and $B_B$ and an effect mediated by the change in the conformations of the amino acid residues and the phytol chain that occur in the presence of carotenoid.

## TRIPLET STATE OF CAROTENOIDS HAVING SHORTER CONJUGATION LENGTHS RECONSTITUTED INTO THE REACTION CENTER OF *Rba. sphaeroides* STRAIN R26.1 AS DETECTED BY TIME-RESOLVED ABSORPTION SPECTROSCOPY

Triplet ($T_1$) energy of P in the RC is determined by using phosphorescence spectroscopy in 1988 [50]. In contrast, there has been no direct measurement of $T_1$ energies of 15,15'-*cis*-carotenoids in any environment. However, the $T_1$ energy level has been predicted to be half that of the singlet ($S_1$, $2^1A_g^-$) energy, based on the PPP-MRD-CI calculations with model polyenes [51]. Recently, the $T_1$ energies of LH2-bound all-*trans* carotenoids, which have the number of conjugated double bonds, $n$ = 11, 10, and 9 have been experimentally determined [52]. The $T_1$ energies increase as $n$ decreases in both cases, although this trend is much stronger in the theoretical prediction. As has already been shown, the carotenoid is bound to the RC with a 15,15'-*cis*-configuration, not all-*trans*. How can we establish the $T_1$ energies of the RC bound 15,15'-*cis*-carotenoid? Farhoosh et al. [16] proposed that the $T_1$ energies of carotenoids having $n$ shorter than 10 are higher than that of $^3B_B$ because no transient absorption nor EPR signal was detected from $T_1$ carotenoids reconstituted into the RC from *Rba. sphaeroides* R26.1. This report conflicts with the previous detection of the $T_1$ absorption spectrum of chloroxanthin ($n$ = 9) bound to the RC from *Rba. sphaeroides* Ga [53]. Since techniques for the reconstitution of the carotenoid into RCs, as well as the detection and/or analysis of the time-resolved absorption spectroscopy, have been much improved since these previous investigations, this issue has been revisited.

The strategy used in the present study was as follows: (1) to use a series of spheroidene analog having different conjugation lengths while conserving the important methoxy group, (2) to assess the

binding of reconstituted carotenoid by using both the usual absorption and CD spectrum and also X-ray crystallography, and (3) to assign the generation of triplet carotenoid precisely by using multichannel detection to record a set of time-resolved absorption spectra, and by applying singular-value decomposition (SVD) in order to extract time-dependent species from the huge data matrix.

### Time-resolved absorption spectroscopy of the RCs

A series of synthetic analogs of spheroidene having $n$ = 11, 9, 8 and spheroidene ($n$ = 10) were reconstituted into the R26.1 RC as previously reported [54]. The wild-type 2.4.1 RC and carotenoidless R26.1 RC were also prepared for comparison. Absorption and CD spectra showed that the binding of the analogs having $n$ = 10, 9, and 8 into the RCs were successful, whereas that of the analog with $n$ = 11 was not.

Time-resolved absorption spectra were recorded as follows: The white light continuum from Ar-$H_2$ lamp (Nano Pulse Light NP 1-A, fwhm 75 ns, Sugawara, Japan) irradiated a quartz cuvette (optical path length, 2 mm) and then the light transmitted through the sample cell, passed through a single monochromator (Spectra-Pro275, Acton Research Corporation, USA) and was detected by a charge-coupled device (CCD) detector (LN/CCD-1340/400-EB1, Roper Scientific, Japan). The excitation pulse from OPO laser (870 nm, 0.18 mJ/pulse, FWHM 5 ns, Spectra-physics MOPO, USA) excited by Nd:YAG laser (355 nm, Quanta-Ray PRO, Spectra-physics) irradiated the cuvette at an angle of ~30º with respect to the probe pulse. The samples of the RCs ($OD_{800}$ ~2 $cm^{-1}$) were deoxygenated as reported previously [16].

### Singular-value-decomposition analysis of the time-resolved absorption spectra of the reconstituted RCs: A functional detection of the carotenoids

Sharp signals due to the $T_1$ state of the carotenoids were clearly detected in the time-resolved absorption spectra of the RCs reconstituted spheroidene analogs having $n$ = 9, 10, 11 on the longer wavelength side of the ground-state bleaching. The $T_1$ signal and the ground-state bleaching of the $n$ = 8 analog could also be identified by carefully comparing it to the $T_1$ absorption spectrum of the R26.1 RC. To confirm this observation, SVD, which is a mathematical method to extract the major changing component from the huge matrix data set, was applied to the full set of time-resolved absorption spectra.

The basis spectra shown in the left panel in Fig. 6 enhance the major components observed in the raw spectra: the sharp $T_1$ signal in the longer wavelength region lies on top of the plateau of the $T_1$ BChl signal and the BChl $Q_x$ bleaching. The time traces of the basis spectra, shown in the right panel in Fig. 6, mainly contain two decay components having short (~5 μs) and long (almost constant in measured temporal region) lifetimes. The former can be assigned to the $T_1$ state of the carotenoid, while the latter to the $T_1$ BChl.

The assignment of the $T_1$ BChl was confirmed by the fact that basis spectrum and its time constant in R26.1 RCs are almost identical to those of the $T_1$ BChl *a* in solution [55]. Mathis and Kleo reported the linear relationship of the $T_n \leftarrow T_1$ and $S_2 \leftarrow S_0$ transition energies of β-carotene analogs having $n$ = 7 – 19 in solution [56]. The peak energies of the $T_n \leftarrow T_1$ absorption of the carotenoids assigned above are also proportional to their main absorption energies, and the slope of the line relating the energies of the measured $T_n \leftarrow T_1$ to the $S_2 \leftarrow S_0$ energies is very similar to that of the β-carotene analogs, confirming the assignment of the $T_1$ absorption of the reconstituted carotenoids.

Therefore, we have concluded that the triplet state of carotenoids with $n$ = 8 or 9 can also be generated by excitation of P. In addition to this, it was also concluded that the SVD analysis of the time-resolved absorption spectra is useful to evaluate the binding of the carotenoid into the RC as a functional detection of carotenoid binding.

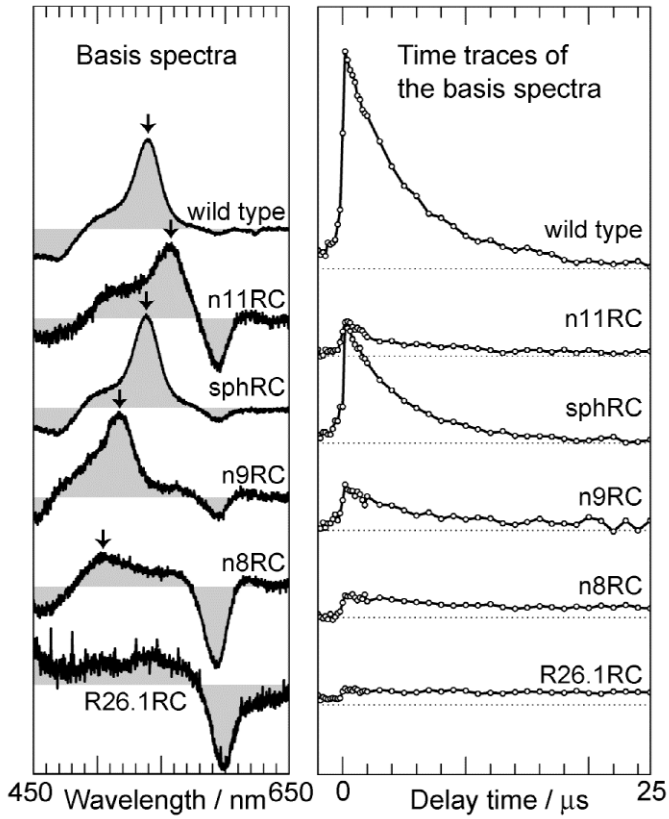


**Fig. 6** The results of the SVD applied to the set of time-resolved absorption spectra of the R26.1 RCs with spheroidene analogs shown in Fig. 2, that without carotenoid and the wild-type 2.4.1 RC excited at 870 nm. The arrows indicate the peaks of transient absorption of $T_1$ carotenoids thus assigned.

## CONCLUSIONS

The structure and function of 15,15'-*cis*-carotenoids bound to the RC from *Rba. sphaeroides* were investigated by using X-ray crystallography, electroabsorption (Stark) spectroscopy, and μs time-resolved absorption spectroscopy.

Upon a precise comparison of the X-ray structure of the carotenoidless RC from *Rba. sphaeroides* R26.1 with that of the spheroidenone-containing RC from *Rba. sphaeroides* AM260W, two differences were found in the region of the carotenoid-binding site: one is the conformational change of Phe M162 in the presence of the carotenoid, the other is the hydrogen bonding between methoxy-oxygen of the carotenoid and hydrogen on the indole N of Trp M75. Upon superimposing the main-chain atoms of the protein in the vicinity of the carotenoid-binding site, the positions of the 15,15'-*cis*-double bond of carotenoids are found to be well conserved while the nonconjugated tail and methoxy head positions differ slightly, among spheroidenone-containing, spheroidene- and 3,4-dihydrospheroidene-reconstituted RCs.

Electroabsorption (Stark) spectroscopy revealed that the static electric field on P due to the presence of carotenoid was estimated to be ~$1 \times 10^5$ [V/cm], which corresponds to approximately 10 % of the total local electric field around P.

Singular-value decomposition analysis of time-resolved absorption changes showed, for the first time, that a reconstituted carotenoid with 8 double bonds could quench the triplet state of P.

## ACKNOWLEDGMENTS

H. H. thanks the grants-in-aid (grant numbers 17204026 and 17654083) from Japanese Ministry of Education, Culture, Sports, Science and Technology. H. H. and R. J. C. thank the support from Strategic International cooperative program by JST and the grant-in-aid from BBSRC. The work in the laboratory of HAF is supported by the National Institutes of Health (GM-30353) and the University of Connecticut Research Foundation. This work is also partially supported by Nakatani Electronic Measuring Technology Association of Japan.

## REFERENCES

1. J. Deisenhofer, O. Epp, K. Miki, R. Huber, H. Michel. *Nature* **318**, 618 (1986).
2. J. P. Allen, G. Feher, T. O. Yeates, D. C. Rees, J. Deisenhofer, H. Michel, R. Huber. *Proc. Natl. Acad. Sci. USA* **83**, 8589 (1986).
3. J. P. Allen, G. Feher, T. O. Yeates, H. Komiya, D. C. Rees. In *The Photosynthetic Bacterial Reaction Center*, J. Breton, A. Vermeglio (Eds.), pp. 5–11, Plenum, New York (1988).
4. B. Arnoux, A. Ducruix, F. Reiss-Hussion, M. Lutz, J. R. Norris, M. Schiffer, C.-H. Chang. *FEBS Lett.* **258**, 47 (1989).
5. C.-H. Chang, D. Tiede, J. Tang, U. Smith, J. R. Norris, M. Schiffer. *FEBS Lett.* **205**, 82 (1986).
6. C.-H. Chang, O. El-Kabbani, D. Tiede, J. R. Norris, M. Schiffer. *Biochemistry* **30**, 5352 (1991).
7. U. Ermler, G. Fritzch, S. K. Buchanan, H. Michel. *Structure* **2**, 925 (1994).
8. G. Feher, J. P. Allen, M. Y. Okamura, D. C. Rees. *Nature* **339**, 111 (1989).
9. H. Komiya, T. O. Yeates, D. C. Rees, J. P. Allen, G. Feher. *Proc. Natl. Acad. Sci. USA* **85**, 9012 (1988).
10. K. E. McAuley, P. K. Fyfe, J. P. Ridge, R. J. Cogdell, N. W. Isaacs, M. R. Jones. *Biochemistry* **39**, 15032 (2000).
11. T. O. Yeates, H. Komiya, A. Chirino, D. C. Rees, J. P. Allen, G. Feher. *Proc. Natl. Acad. Sci. USA* **85**, 7993 (1988).
12. A. W. Roszak, K. McKendrick, A. T. Gardiner, I. A. Mitchell, N. W. Isaacs, R. J. Cogdell, H. Hashimoto, H. A. Frank. *Structure* **12**, 765 (2004).
13. H. A. Frank, R. J. Cogdell. In *Carotenoids in Photosynthesis*, A. Young, G. Britton (Eds.), pp. 253–326, Chapman & Hall, London (1993).
14. H. A. Frank, C. A. Violette. *Biochim. Biophys. Acta* **976**, 222 (1989).
15. H. A. Frank, V. Chynwat, A. Posteraro, G. Hartwich, I. Simonin, H. Scheer. *Photochem. Photobiol.* **64**, 823 (1996).
16. R. Farhoosh, V. Chynwat, R. Gebhard, J. Lugtenburg, H. A. Frank. *Photochem. Photobiol.* **66**, 97 (1997).
17. K. Yanagi, M. Shimizu, H. Hashimoto, A. T. Gardiner, A. W. Roszak, R. J. Cogdell. *J. Phys. Chem. B* **109**, 992 (2005).
18. P. Wang, R. Nakamura, Y. Kanematsu, Y. Koyama, H. Nagae, T. Nishio, H. Hashimoto, J.-P. Zhang. *Chem. Phys. Lett.* **410**, 108 (2005).
19. A. J. Chirino, E. J. Lous, M. Huber, J. P. Allen, C. C. Schenck, M. L. Paddock, G. Feher, D. C. Rees. *Biochemistry* **33**, 4584 (1994).
20. J. W. Ponder, F. M. Richards. *J. Mol. Biol.* **193**, 775 (1987).
21. T. Sashima, L. Limantara, Y. Koyama. *J. Phys. Chem. B* **104**, 8308 (2000).
22. B. Arnoux, J.-F. Gaucher, A. Ducruix, F. Reiss-Hussion. *Acta Crystallogr., Sect. D* **51**, 368 (1995).
23. S. Lin, E. Katilius, A. K. W. Taguchi, N. W. Woodbury. *J. Phys. Chem. B* **107**, 14103 (2003).
24. A. Angerhofer, F. Bornhauser, V. Aust, G. Hartwich, H. Scheer. *Biochim. Biophys. Acta* **1365**, 404 (1998).

25. N. J. Fraser, H. Hashimoto, R. J. Cogdell. *Photosynth. Res.* **70**, 249 (2001).
26. T. O. Yeates, H. Komiya, D. C. Rees, J. P. Allen, G. Feher. *Proc. Natl. Acad. Sci. USA* **84**, 6438 (1987).
27. T. R. Middendorf, L. T. Mazzola, K. Lao, M. A. Steffen, S. G. Boxer. *Biochim. Biophys. Acta* **1143**, 223 (1993).
28. W. Liptay, R. Wortmann, H. Schaffrin, O. Burkhard, W. Reitinger, N. Detzer. *Chem. Phys.* **120**, 429 (1988).
29. W. Liptay. In *Excited States*, E. C. Lim (Ed.), pp. 129–229, Academic Press, New York (1974).
30. L. M. P. Beekman, R. N. Frese, G. J. S. Fowler, I. Ortiz de Zarate, R. J. Cogdell, I. van Stokkum, C. N. Hunter, R. van Grondelle. *J. Phys. Chem. B* **101**, 7293 (1997).
31. L. M. P. Beekman, M. Steffen, I. van Stokkum, J. D. Olsen, C. N. Hunter, S. G. Boxer, R. van Grondelle. *J. Phys. Chem. B* **101**, 7284 (1997).
32. H. P. Braun, M. E. Michel-Beyerle, J. Breton, S. Buchanan, H. Michel. *FEBS Lett.* **221**, 221 (1987).
33. P. Eisenberger, M. Y. Okamura, G. Feher. *Biophys. J.* **37**, 523 (1982).
34. T. J. DiMagno, E. J. Bylina, A. Angerhofer, D. C. Youvan, J. R. Norris. *Biochemistry* **29**, 899 (1990).
35. D. S. Gottfried, M. A. Steffen, S. G. Boxer. *Biochim. Biophys. Acta* **1059**, 76 (1991).
36. S. L. Hammes, L. Mazzola, S. G. Boxer, D. F. Gaul, C. C. Schenck. *Proc. Natl. Acad. Sci. USA.* **87**, 5682 (1990).
37. D. J. Lockhart, S. G. Boxer. *Biochemistry* **26**, 664 (1987).
38. D. J. Lockhart, S. G. Boxer. *Proc. Natl. Acad. Sci. USA* **85**, 107 (1988).
39. M. Losche, G. Feher, M. Y. Okamura. *Proc. Natl. Acad. Sci. USA* **84**, 7537 (1987).
40. M. A. Steffen, K. Lao, S. G. Boxer. *Science* **264**, 810 (1994).
41. K. Yanagi, H. Hashimoto, A. T. Gardiner, R. J. Cogdell. *J. Phys. Chem. B* **108**, 10334 (2004).
42. H. Zhou, S. G. Boxer. *J. Phys. Chem. B* **102**, 9148 (1998).
43. H. Zhou, S. G. Boxer. *J. Phys. Chem. B* **102**, 9139 (1998).
44. L. J. Moore, H. Zhou, S. G. Boxer. *Biochemistry* **38**, 11949 (1999).
45. K. Lao, L. J. Moore, H. Zhou, S. G. Boxer. *J. Phys. Chem.* **99**, 496 (1995).
46. S. G. Boxer. In *Biophysical Techniques in Photosynthesis*, S. G. Boxer (Ed.), pp. 177–189, Kluwer Academic, Dordrecht, (1996).
47. S. G. Boxer, R. A. Goldstein, D. J. Lockhart, T. R. Middendorf, L. Takiff. *J. Phys. Chem.* **93**, 8280 (1989).
48. M. Kohler, J. Friedrich, J. Fidy. *Biochim. Biophys. Acta* **1386**, 255 (1998).
49. P. O. J. Scherer, S. F. Fischer. *Chem. Phys. Lett.* **131**, 153 (1986).
50. L. Takiff, S. G. Boxer. *J. Am. Chem. Soc.* **110**, 4425 (1988).
51. P. Tavan, K. Schulten. *Phys. Rev. B* **36**, 4337 (1987).
52. F. S. Rondonuwu, T. Taguchi, R. Fujii, K. Yokoyama, Y. Koyama, Y. Watanabe. *Chem. Phys. Lett.* **384**, 364 (2004).
53. R. J. Cogdell, T. G. Monger, W. W. Parson. *Biochim. Biophys. Acta* **408**, 189 (1975).
54. H. A. Frank. In *The Photochemistry of Carotenoids*, H. A. Frank, A. J. Young, G. Britton, R. J. Cogdell (Eds.), pp. 235–244, Kluwer, Dordrecht, (1999).
55. E. Nishizawa, H. Nagae, Y. Koyama. *J. Phys. Chem.* **98**, 12086 (1994).
56. P. Mathis, J. Kleo. *Photochem. Photobiol.* **18**, 343 (1973).